DOE/ER-0045/5

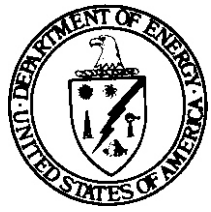

Alloy Development for Irradiation Performance

Quarterly Progress Report
For Period Ending December 31,1980

U.S. Department of Energy
Office of Fusion Energy

CONTENTS

FOREWORD.. iii

1. ANALYSIS AND EVALUATION STUDIES 1

1.1 Materials Handbook for Fusion Energy Systems (McDonnell Douglas Astronautics Company and Hanford Engineering Development Laboratory) 2

The data sheets and the revision of the existing pages in the handbook are proceeding satisfactorily. The bulk of the property sheets relate to properties of type 316 austenitic stainless steel which were prepared in support of the ETF design. Data sheets covering fatigue cmck growth, swelling, and physical properties have been submitted to the ADIP task group for review. The data sheets describing the effects of irmdiation in elevated tern perature fatigue strength of 20% cold worked 316 have been reviewed and approved by both ADIP and A&E tusk groups and wilt be included in the first publication package of the MHFES. Data sheets in preparation but not submitted to the respective task groups for approval are: effect of irradiation on the mechanical properties of 20% cold worked 316; Structuml properties of stainless steel alloys for magnet cases; and properties of glass laminates for superconducting rmgnet insulators.

2. TEST MATRICES AND TEST METHODS DEVELOPMENT 5

2.1 Status of MFE-5 In-Reactor Fatigue Crack Growth Experiment (Hanford Engineering Development Laboratory) . . 6

The in-reactor fatigue rmchine has been inserted into the ORR and cycling on a chain of 20% cold-worked 316 stainless steel specimens has commenced. Because of the uncertainties in the y-heating profile, the tempemture profile across the specimen chain could not be optimized. However, this temperature profile was duplicated for the thermal control test, and cycling on this second chain of specimens has been initiated at HEDL.

2.2 Neutronic Calculations for the Conceptual Design of an In-Reactor Solid Breeder Experiment, TRIO-01 (Oak Ridge National Laboratory) 10

Two-dimensional transport calculations of the TRIO-01 breeder experiment have been performed and the results of these calculations have been compared with previously generated one-dimensional results. The two-dimensional results indicate approxirmtely 5% decrease in the tritium production and less than 20% decrease in the heating mtes within the experimental rmterials.

The change in the thermal flux and the flux above thermal along the poolside face due to the insertion of the TRIO-01 experiment in position A2 of the ORR has been estimated using VENTURE and a simulated model of the experiment. The ^{6}Li and ^{7}Li cross sections needed to adequately describe the experiment using VENTURE have been processed and better estimates of the flux change due to the insertion of the experiment are being obtained.

A report entitled "Neutronics Calculations for the Conceptual Design of an In-Reactor Solid Breeder Experiment, TRIO-01," covering the one dimensional neutronics calculations has been prepared and is being reviewed.

2.3 Neutronic Calculations in Support of the ORR-MFE-4 Spectral Tailoring Experiment (Oak Ridge National Laboratory) . . . 15

Three-dimensional neutronic calculations are being carried out to follow the irmdiation environment of the ORR-MFE-4A experiment. These calculatiuons currently cover the 15 ORR reactor cycles completed to December 12, 1980, corresponding to 111,466 MWh, 3.45 x 10^{25} neutrons/m^2 in thermal fluence and 1.03 x 10^{26} neutrons/m^2 in total fluence. This produces 2.61 dpa and 25.75 at. ppm He in type 316 stainless steel (not including 2.0 at. ppm He from ^{10}B). Using these data and previous calculations, real time projections have been rmde to estimate the dates that the core pieces should be changed and first samples removed.

The preliminary calculations to determine the appropriate sizes of the hafnium core pieces have been accomplished, and in addition, the heating mtes within the experimental capsules have been obtained. For a given reduction in thermal flux, the decrease in gamma heating due to the use of either hafnium or tungsten core pieces does not drastically differ. Since the thickness of hafnium needed to obtain a specified thermal flux reduction is approximately me-fourth the thickness of tungsten needed, the reduction in gamma heating is most likely due to a loss of fission gams and not due to gamma attenuation in the core pieces. Catcutations are currently in progress to validate this statement.

3. PATH A ALLOY DEVELOPMENT — AUSTENITIC STAINLESS STEELS 19

3.1 High Temperature Fatigue Crack Propagation of Type 316 Stainless Steel in Vacuum (Naval Research Laboratory) . . . 20

Elevated temperatures fatigue crack propagation tests have been conducted in vacuum on specimens of MFE and FBR reference annealed Type 316 stainless steel. The MFE alloy was tested at 550°C and the FBR alloy at 550 and 593°C.

For the levels of ΔK employed in these experiments (ΔK < 33 MPa √m), the mtes of fatigue crack propagation in vacuum were significantly lower than those of the FBR steel tested in air at 593°C.

3.2 Design and Fabrication of Preirradiation Microstructures in Path A Prime Candidate Alloy (Oak Ridge National Laboratory) 25

Previous work described seven desired preirradiation microstructures and six of these were successfully produced in specimen mterial with a coarse (ASTM 1-3) grain size. The seventh microstructure, which consists of fine MC precipitates at the grain boundaries and within grains together with a high dislocation density, was not successfully produced initially. However, with modification of the TMTs, this microstructure has been successfully produced in coarse-grain material. Five of the seven microstructures were identified for production in finer grain material (ASTM 7-8). The fabrication sequences and TMTs were adjusted to reduce the grain size without significant MC precipitation prior to the final TMTs and without losing the homogeneity achieved in coarse grained material. A uniform fine grain size was achieved by reducing the temperature of the final 15-min solution anneal from 1175 to 1100°C. The homogeneity was slightly perturbed by this treatment, but the final microstructures with variable distributions of MC precipitate both at the grain boundaries and in the matrix resulted. This completes Phase I of alloy development in Path A PCA.

3.3 Swelling and Microstructure of HFIR-Irradiated 20%-Cold-Worked Type 316 Stainless Steel (Oak Ridge National Laboratory) 43

Swelling and microstructural results were obtained for CW 316 and CW 316 + Ti after HFIR irradiation at temperatures of 55 to 670°C and to neutron fluences producing 7.7 to 10.8 dpa and 380 to 520 at. ppm He. Cavities and swelling were observed at 285°C and above in CW 316. No cavities could be detected (for d > 2 nm) at 55°C. The swelling in all cases is below 0.5%. Within this limit there is considemble temperature dependence of the microstructure. Swelling in CW 316 is maximum at 285°C and minimum at about 450 to 550°C. The cavities are equilibrium bubbles at 375°C and above, but appear to be voidtike at 285°C. Gmin-boundary cavities are visible between 475 and 565°C and contribute to swelling at 565°C and above. Immersion density measurements confirm the temperature dependence of the cavity volume fraction swelling but the magnitude is lower, probably reflecting densification. Both measurements indicate less swelling in the CW 316 + Ti at most temperatures. The MC interfacial helium trapping

reduces the swelling at 375°C and above. Trapping by MC precipitate particles results in nwre smaller cavities and less swelling. We conclude that the helium ha6 a strong effect on microstructural evolution for these irradiation conditions.

4. PATH B ALLOY DEVELOPMENT — HIGHER STRENGTH Fe–Ni–Cr ALLOYS . . . 71

No contributions.

5. PATH C ALLOY DEVELOPMENT — REACTIVE AND REFRACTORY ALLOYS . . . 73

5.1 The Effect of Hydrogen on Flaw Growth of Titanium Alloy Ti–62425 (McDonnell Douglas Astronautics Company) . . 74

Additional fatigue crack growth rate tests have been conducted at room tempemture in a vacuum on Ti–6242s samples with 500 wppm internal hydrogen. At high stress intensities the fatigue crack growth mte increased with decreasing frequency.

5.2 Titanium Alloy Tensile Properties After Neutron Irradiation (*Hanford* Engineering Development Laboratory) 77

Irradiated specimens from three titanium alloys (6242S, 5621S, Ti–6A1–4V) were tested in uniaxial tension in air from room temperature to 550°C. Each alloy was in a duple—annealed condition. The strain mte during testing was 4.2 × 10^{-5} s^{-1}. The EBR–II irradiation temperature was 550°C; the maximum fluence was 5 × 10^{22} n/cm^2 (E>0.1 MeV) or 24 dpa. The specimens were from the first of three capsules from the AD-1 experiment. The remaining two had irradiation temperatures of 394 and 450°C; tensile tests will be performed on material from these capsules in the near future.

Alloy 6242S increased in strength because of reactor exposure by approximately 20% at test temperatures from room to 400°C. Ductility losses of up to 75% were found.

The strength of 5621S seemed to be unaffected by reactor exposure while its ductility was reduced from that of unirradiated nuterial by up to 80%.

Ti–6Al–4V displayed strength reductions at 550°C test tempemture with nearly an 80% reduction in total elongation.

While large ductility losses were noted after reactor exposure, reasonable postirradiation ductility remained in the specimens. Total elongations mnged from ~1–9%.

All of the specimens had some degree of corrosive attack, which probably occurred during cleaning after reactor discharge. The corrosion ranged from discoloration to

loss of mterial. Although specimens with the least corrosion were chosen for testing, the mechanical properties could include corrosion effects as well as irradiation effects. Hence, the ductilities and ultimate strengths obtained in this study are minimum values.

5.3 Mechanical Property Evaluations of Path C Vanadium Scoping Alloys (Westinghouse Electric Corporation) **92**

Sheet rmteriat of the Path C vanadium Scoping Alloys has been procured from the ETM Research Materials Stockpile and subjected to preliminary recrystallization studies. Based on optical metallography and hardness measurements, a fine, equiaxed 1–30 µm grain size) microstructure results from one hour heat treatments at 1100, 1200, and 1350°C for the V-20Ti, V-15Cr-5Ti, and VANSTAR-7 alloys, respectively. Machining of specimens for tensile and creep-rupture testing has been initiated.

5.4 Fatigue Behavior of Path C Vanadium Scoping Alloys (Oak Ridge National Laboratory) **98**

Limited test data obtained from fully reversed cyclic fatigue tests on unirradiated Vanstar-7 (ADIP heat CAM-836 T-6) at room temperature and 650°C fell consistently below the average trend curves of V–15% Cr–5% Ti tested at the corresponding temperatures. It appears that V–15% Cr–5% Ti has superior fatigue resistance to Vanstar-7.

5.5 Initial Observation of Voids in Neutron Irradiated Titanium Alloys (Hanford Engineering Development Laboratory) **103**

A preliminary transmission electron microscopy examination of Ti-6242S irradiated to 5.0 x 10^{22} n/cm^2 *(E >0.1 MeV) at 550°C has revealed the presence of voids in this near-alpha alloy. The voids were observed only in the primary alpha grains and do not constitute a large volume fraction.*

6. PATH D ALLOY DEVELOPMENT — INNOVATIVE MATERIAL CONCEPTS **107**

6.1 Development of Iron Base Alloys with Long-Range Ordered Crystal Structure (Oak Ridge National Laboratory) **108**

The iron-base LRO alloys with base compositions $(Fe,Ni)_3V$ *are being developed for fusion energy applications. The base alloys are also modified with less than 1% Ti for further improvement in metallurgical and mechanical properties. We have found that the phase relation in the LRO alloys depends strongly on the nickel concentration. The disordered face-centered cubic (fcc) solid solution (gamma phase) starts to precipitate sigma phase at*

1000°C in the 32% Ni–0.9% Ti alloy, and γ + σ phase field extends down to the critical ordering temperature, T_c = 690°C. The existence of the sigma phase (σ), with tetragonal crystal structure, is not desirable, because, in some cases, the retention of the σ phase below T_c lowers the ductility and weakens atomic order in the alloys. The sigma phase region can be eliminated by increasing the nickel content to 40%. The LRO alloys show excellent creep resistance and structural stability. Long-term aging at 550°C does not cause any significant change in the tensile properties of the LRO alloys. The creep rate of the LRO alloys is lower than that of annealed type 316 stainless steel by more than 3 orders of magnitude. Ingots of the 40%Ni–0.4% Ti alloy were prepared by using commercially produced ferrovanadium, to lower the mterial cost. The heats prepared from ferrovanadium show finer grain structure and higher yield strength, compared to the heat prepared from pure vanadium. The ferrovanadium heats are ductile, with tensile elongation exceeding 30% at all test temperatures.

6.2 The Effect of 4-MeV Nickel Ion Irradiation on the Microstructure of $(Fe,Ni)_3V$ Long-Range Ordered Alloys (Oak Ridge National Laboratory) 119

Additional data for ion bombarded $(Fe,Ni)_3V$ LRO alloys show convincingly that ordering is an important factor in the resistance of this alloy class to swelling resulting from cavity formation. Relatively low swelling was observed as long as the irradiation tempemture was below T_c (~670°C). Swelling increased rapidly above T_c. Small titanium additions improved and the presence of sigma phase degraded the resistance to swelling in the LRO-16/LRO-35 alloy series. Similar effects could not be defined for alloy pairs with a higher nickel content.

7. PATH E ALLOY DEVELOPMENT — FERRITIC STEELS 123

7.1 Initial Characterization of the 12Cr Fusion Ferritic Program Heat (General Atomic Company) 124

7.2 Fracture Resistance Testing of Alloy HT-9 in the Unirradiated Condition (Naval Research Laboratory) 127

Alloy HT-9, a 12 Cr martensitic stainless steel, is being evaluated for potential applications as a first wall material in magnetic fusion reactors and as a duct material for fast breeder reactors. The present study examined the notch ductility and static fmcture toughness of material from two HT-9 melts (melt numbers 91353 and 91354) in the unirradiated condition.

Material comparisons revealed a potential for large differences in Charpy-V (C_v) notch ductility both in terms of upper shelf energy level and in terms of brittle/ductile transition temperature. The transition temperature of one 15.9 mm plate from melt 91353 exceeded 200°C, while the transition temperature for a 33 mm rod from melt 91354 was −18°C. Large variations in J-R curve behavior were also observed, the probable cause of which is inadvertent differences in rmterial heat treatment. The observed material variability m y explain why difficulties were encountered in duct fabrication. A reheat treatment of the 15.9 mm plate was found to improve notch ductility properties greatly.

7.3 Preparation of Alloy HT-9 **Reference Plate for Irradiated Fracture Resistance Studies (Naval Research Laboratory) . . 142**

To be reported in the next quarterly report.

7.4 The Microstructural Evaluation of **Embrittled 12Cr-1Mo-0.3V Steel (General Atomic Company) 143**

This section reviews the initial work already reported to determine the effect of embrittlement on the fracture properties (CVN and K_{Id}) of HT-9. Also included is a sum mry of the new data evaluating the microstructures of the embrittled alloy.

Earlier, the dynamic stress intensity factor, K_{Id}, and Charpy impact energy (CVN) transition temperature curves were determined for a 12Cr-1Mo-0.3V steel (HT-9). The specific heat treatment was determined by observing the effect of austenitizing and tempering temperatures on prior austenite grain sizes, hardness, and carbide precipitation. It was concluded that a treatment of 1000°C for an hour followed by an air-cool and subsequent tempering at 650°C for an hour produced a microstructure nearly as stable as the higher temperature industrially recommended heat treatment. Specimens for fracture properties were thus treated, then half were aged at 550°C for 100 hours to induce embrittlement. The ductile-to-brittle transition temperature (DBTT) for each condition was determined. There was an 80°C increase in the DBTT measured by instrumented and precracked CVN, whereas the standard blunt notched CVN showed no shift. The fracture surfaces in both cases were quasi-cleavage along martensite lath boundaries with no indication of intergranular decohesion. Since the fracture properties were measured, a transmission electron microscopic examination of the microstructures of the as-quenched (AQ), quenched and tempered (Q+T), and Q+T and aged conditions have been performed. It was found that

thin films (~200Å) of austenite were retained at the martensite lath boundaries after air-cooling from the austenitizing temperature. Upon tempering, these films transform to $M_{23}C_6$ discontinuous carbide networks (an presumabty ferrite), and the martensite kzths evidence some sub-grain formation within the kzths. Subsequent aging at 550°C for 100 hours produced a small increase in volume percent of stable $M_{23}C_6$ and tittle change in other fine microstructural details.

7.5 Environmental Effects on Properties of Ferritic Steels (Argonne National Laboratory) 156

Several continuous-cycle fatigue tests have been conducted with 2.5-mm-diameter specimens of HT-9 alloys at 755 K in a lithium environment of controlled purity. However, the fatigue test program was temporarily suspended because of a gradual increase in the nitrogen content of the lithium. The lithium loop was shut down twice owing to plugging of the cold-trap purification loop. Metallogmphic examination of the cold-trap pipe indicates that plugging was caused by trapping of nickel-manganese and iron-nickel-manganese crystals under the pump coil and flowmeter magnet. The increased nitrogen concentration in the 'lithium resulted in excessive corrosion and mass transfer. The nitrogen in the lithium also had a large effect on the fatigue behavior of the HT-9 alloy. Metallographic evaluation of HT-9 alloy, Type 316 stainless steel, and Inconel 625 exposed in contact with solid Li_2O, $LiAlO_2$, and Li_2SiO_3 breeding materials has been completed. Results indicate that Li_2O is the most reactive of the three breeding materials. HT-9 alloy exposed in contact with Li_2O contained Li_5FeO_4 and $LiCrO_2$ compounds, whereas $Li_2Ni_8O_{10}$ and $LiCrO_2$ were observed on Inconel 625. The presence of these volatile compounds may explain the higher reactivity of Li_2O.

7.6 Fabrication of Materials for the RB-1 Experiment in HFIR (Hanford Engineering Development Laboratory) 170

Selected ferritic alloys have been mechanically processed for use in the fabrication of specimens for the MFE-RB-1 experiment in HFIR and for the reencapsulation of the AD-2 experiment in EBR-II. Weldments have been fabricated from HT-9, modified 9Cr-1Mo, and 2-1/4Cr-1Mo base metals.

7.7 Microstructural Examination of a Series of Commercial Ferritic Alloys Irradiated to Very High Fluence (Hanford Engineering Development Laboratory) 187

A series of five commercial ferritic alloys 21/4Cr-1Mo, H-11, EM-12, 416, and 430F, covering the

composition mnge 2.25 to 17% chromium and including a wide range of preirmdiation microstructures has been examined by transmission electron microscopy following irmdiation in the EBR-II over the temperature mnge 400-650°C and to a maximum fluence of 17.6 × 10^{22} n/cm^2 (E >0.1 MeV) or 84 dpa. These materials were confirmed to be low void swelling with nuximum swelling of 0.63% measured in EM-12 following irradiation at 400°C to 14.0 × 10^{22} n/cm^2. A wide range of precipitation response was found in these materials both as a function of alloy and irradiation tempemture. Precipitates observed included M_6C, Mo_2C, Chi, Laves, $M_{23}C_6$, α´ and a low tempemture phase as yet unidentified. It is predicted, based on these results, that the major impact of irmdiation on the ferritic alloy class will be changes in postirradiation mechanical properties due to precipitation.

7.8 Microstructural Examination of HT-9 Archive Material from the AD-2 Test (Hanford Engineering Development Laboratory) 212

The HT-9 fmcture toughness and miniature Charpy specimens included in the AD-2 test received a different set of thermomechanical treatments (TMTs) than the tensile, cmck growth and Grodzinski fatigue specimens. Tmnsmission electron microscopy (TEM) has been performed on material stock representing the four treatments involved. All four treatments produced essentially identical tempered martensite structures.

7.9 Tensile Properties of Three Ferritic Steels after Low-Temperature HFIR Irradiation (Oak Ridge National Laboratory) 218

Tensile specimens from small heats of ferritic (martensitic) steels based on 12 Cr-1 MoVW, 9 Cr-1 MoVNb, and the low-attoy ferritic 2 1/4 Cr-1 Mo steel have been irradiated to displacement damage levels of up to about 9 dpa in HFIR. The 12 Cr-1 MoVW- and 9 Cr-1 MoVNb-base compositions were irmdiated, along with similar alloys to which nickel had been added. Transmutation of the ^{58}Ni during irradiation in HFIR can lead to helium production rates similar to those anticipated in a fusion reactor. Displacement damage is produced simultaneously by the fast neutron flux in the reactor.

During the present reporting period, irradiated specimens from two heats of 12 Cr-1 MoVW and three heats of 12 Cr-1 MoVW with 1 and 2% Ni were tensile tested at mom tempemture and 300°C. Yield strength and ultimate tensile strength of irmdiated samples displayed considerable hardening over the unirradiated condition. The increased

strength was accompanied by a decrease in ductility. Indications are that the hardening resulted only from the displacement damage, and was not affected by the transmutation helium formed during irradiation.

7.10 Immersion Density Analysis of Commercial Alloys Irradiated to a Very High Fluence (Hanford Engineering Development Laboratory) 226

Immersion density measurements have been performed on a series of high-nickel, refractory and ferritic commercial alloys irradiated in EBR-II to a peak fluence of 17.8 × 10^{22} n/cm^2 (E >0.1 MeV). The specimens were irradiated at temperatures ranging from 400 to 650°C. All of the alloys exhibit swelling resistance far superior to AISI 316. None of the ferritic alloys exhibited more than 5.6% swelling after this high exposure.

The high-nickel superalloys, Inconel X-750 and Inconel 718, both show a low temperature swelling peak. Inconel X-750 swells more than Inconel 718 at all temperatures and has a peak of 2.4% at 427°C.

The refractory alloys, TZM and Nb-1Zr, both show peak swelling at temperatures at or above 593°C. TZM exhibits the greatest swelling with a peak of 3.6% at 593°C.

8. STATUS OF IRRADIATION EXPERIMENTS AND MATERIALS INVENTORY . . . 235

8.1 Irradiation Experiment Status and Schedule (Oak Ridge National Laboratory) 236

Principal features of many ADIP irradiation experiments are tabulated. Bar charts show the schedule for recent, current, and planned experiments. Experiments are presently under way in the Oak Ridge Research Reactor (ORR) and the High Flux Isotope Reactor (HFIR), which are mixed spectrum reactors, and in the Experimental Breeder Reactor (EBR-II), which is a fast reactor.

8.2 ETM Research Materials Inventory (Oak Ridge National Laboratory) 243

The Office of Fusion Energy has assigned program responsibitity to ORNL for the establishment and operation of a central inventory of research materials to be used in the Fusion Reactor Materials research and development programs. The objective is to provide a common supply of material for the Fusion Reactor Materials Program. This will minimize unintended materials variables and provide for economy in procurement and for centralized record-keeping. Initially this inventory will focus on materials related to first-wall and structural applications and related research, but various special purpose materials my be added in the future.

9. MATERIALS COMPATIBILITY **AND** HYDROGEN PERMEATION STUDIES **249**

9.1 Compatibility **of** Ferritic Steels with Static Lithium and **Li–5 wt %** Al (Oak Ridge National Laboratory) **250**

Exposures of HT9 to static 500°C lithium for up to 3000 h resulted in negligible weight changes and did not significantly affect the steel's room temperature tensile properties relative to specimens exposed to argon under otherwise similar conditions. Gage sections of 2 1/4 Cr–1 Mo steel specimens exposed for 3000 h to Li–5 **wt %** *Al at 500 and 600°C cracked severely when these specimens were tensile tested at mom temperature. Type 316 stainless steel did not deteriorate mechanically when exposed to Li-5 wt % Al for 1000 h at 500°C. Aluminum was incorporated into surface layers on the alloys and appears to have blocked the normal decarburization of 2 1/4 Cr–1 Mo steel in lithium.*

9.2 Corrosion **of** Type **316** Stainless Steel and a Long-Range-Ordered Fe–Ni–V Alloy in Naturally Convective Lithium (Oak Ridge National Laboratory) **256**

Further results on corrosion mtes of type 316 stainless steel in lithium-type 316 stainless steel thermal-convection loops (TCLs) are given. The mtes in one loop were significantly lower than those measured in several other similar experiments. Comparison of exposed coupons showed that all surfaces experiencing dissolution exhibited porosity, but those with the lower corrosion rates had shallower porous layers. The cause of the lower corrosion mtes has not been established but does not appear to be associated with the purity of the lithium. Additionally, data on the corrosion mtes of long-range-ordered (LRO) alloy Fe–31.8 Ni–22.5 V–0.4 Ti (wt %) exposed in lithium-type 316 stainless steel TCLs are reported. These mtes, which include a contribution from dissimilar-metal transfer of nickel from the alloy, are significantly greater than those of type 316 stainless steel previously exposed in these toops.